Chapter 1
XRF-Basics

Abstract This chapter describes the main interactions of X-rays with matter and how these can be used for the characterization of material. Such interactions are absorption, emission of fluorescence (or secondary) radiation, refraction, scattering and diffraction. This discussion will be limited because there are several papers and even monographs which describe these interactions very detailed. An overview of the main components of an X-ray spectrometer with their expected functionality is provided at the end of the chapter.

1.1 Introduction

X-Ray fluorescence is now an established analytical method for the examination of the elemental composition of bulk material and also for the characterization of coating systems. It covers a broad range of elements and can handle a widespread weight fraction range from traces to pure elements. The physical form of analyzed samples ranges from solid sample to powders or particles and also liquids. The measured sample itself is not influenced by the measurement procedure i.e. the analysis within the measuring system is non-destructive and the samples can be archived for further investigations.

However, the analyzed material often has to be 'destructively' prepared by cutting, grinding, deformation or polishing in case of the analysis of large sample areas to get homogeneous samples which then represents the material that has to be characterized or to get a sample that fits into the sample holder of the instrument. But very often not the composition of the homogenized material is of interest but rather the investigation of the inhomogeneous composition of products. And this should be possible by a non-destructive analysis. This analytical task can be solved by micro-X-ray fluorescence.

μ-XRF had a strong development in the last 10–15 years. The high interest in this method for position sensitive elemental analysis can be understood because of the increasing demands for analysis of composites of diverse materials with

M. Haschke, *Laboratory Micro-X-Ray Fluorescence Spectroscopy*,
Springer Series in Surface Sciences 55, DOI: 10.1007/978-3-319-04864-2_1,

differing composition. These inhomogeneous materials cause macroscopic properties like mechanic, electric, magnetic, optic properties etc. which define the function of final products. Consequently, considerable effort is spent for the characterization of basic products and the improvement of manufacturing technologies but also the final products needs to be correctly analyzed—both for the warranty of their functionality or for failure analysis. If the primary products very often can be prepared in a homogeneous form this is not possible for final products.

Another reason for the requirement to analyze a small sample area can be the shape of final products. If they are not flat or have a shape which cannot be positioned in the sample chamber of an instrument, a section of the item needs to be taken for a measurement, necessitating damage of the product.

These requirements are very well managed by μ-XRF. Their excitation of small sample areas allows the analysis of inhomogeneous samples—both of special sample areas but also the distribution of elements in one or two dimensions i.e. over lines or areas, and for special samples even for a 3-dimensional element distribution. And this analytical performance is available even with an easy sample handling and a simple sample preparation.

For that purpose the excitation radiation has to be concentrated to a small sample area which then has to give sufficient signal intensity. The mentioned expeditious development of this method in the last years was mainly initiated by the availability of X-ray optics that allow the efficient excitation of small sample areas to give a sufficient fluorescence intensity for a satisfying signal.

The excitation of a small sample area requires primary optics between source and sample that shapes the beam. There are different X-ray optics available which have beam shaping functions but mostly they also influence the spectral distribution of the beam. The selection of the best X-ray optic for a certain application therefore is very important.

Other requirements arise from the correct sample positioning. If non-homogeneous or, in particular, non-regular shaped samples has to be analyzed it is necessary that the area or interest can be easily and correctly positioned. For very small analyzed sample areas it is even necessary to control this position, for example, with a magnified sample view. Also the detection of X-ray fluorescence has to be considered—high acceptance angle, good energy resolution and high count rates are required.

The first experiments for spatial resolved X-ray fluorescence were performed on synchrotrons [1, 2]. Their high primary intensity could be used in connection with small collimators [3–7] to generate small beam diameters which could be used for the excitation of fluorescence radiation. By using X-ray optics the excitation intensity could be even increased combined with a reduction of spot size i.e. the analytical performance could be improved [8–14]. The excitation of X-ray fluorescence by X-ray tubes is used for a long time. At the beginning the analyzed areas were large to get sufficient excitation intensity, in particular by the wavelength dispersive spectrometers which were available only at that time [15–18].

The excitation of small sample areas was realized at the beginning only with collimators [19–26]. But this was limiting the excitation intensity even in case of using high power X-ray tubes with rotating anodes [27] which was restricting also the analytical performance. Smaller spots with higher intensities could be realized with X-Ray optics only. The properties of capillaries for the propagation of X-Rays were investigated already in the 1970s [28, 29]. With the availability of X-ray optics, in particular of capillary optics also smaller spots was possible and then μ-XRF could be performed also with laboratory instruments. The first instruments were prepared with mono-capillaries [30–34]. In this case the spot size could be already very small, down into the 5 µm range [34, 35] but the measured intensities was also very low. The availability of poly-capillary optics then offers the combination of small spots—at the beginning down to 40–50 µm—with high excitation intensity which allows the use of this technique also for laboratory instrumentation [36–42].

New components for μ-XRF methods as well as new applications often are tested at first on synchrotron sources and only then they are transferred to laboratory instruments. This is valid for the introduction of X-ray optics but also for other technologies, quantification methods and a wide range of applications. Also nowadays synchrotrons are used for more sophisticated investigations, for example with higher spatial resolution or flexible excitation conditions. But their limited availability and high effort for the examination requires also the availability of laboratory instruments for the general daily use.

Therefore this book concentrates only on the description of laboratory instruments because meanwhile they are available in a lot of laboratories and with different instrumental concepts—both as prototypes in research laboratories but also as commercially available instruments. This enables their use nowadays for a wide range of different applications.

A more detailed discussion of μ-XRF with synchrotron radiation and a comparison of differences in analytical performance will follow in 6.1.1.

1.2 Interaction of X-rays with Matter Used for Material Characterization

Already a short time after the discovery of X-rays there was several attempts to use this form of radiation for the characterization of material.

The short wavelengths of this radiation which is in the range of the atomic distances in solid and liquid material and the high penetration into material offers different possibilities for the examination of material. There are different interactions of X-rays with material that can be used—absorption, scattering or diffraction, refraction and emission [for example 43–48]. These interactions are schematically displayed in Fig. 1.1.

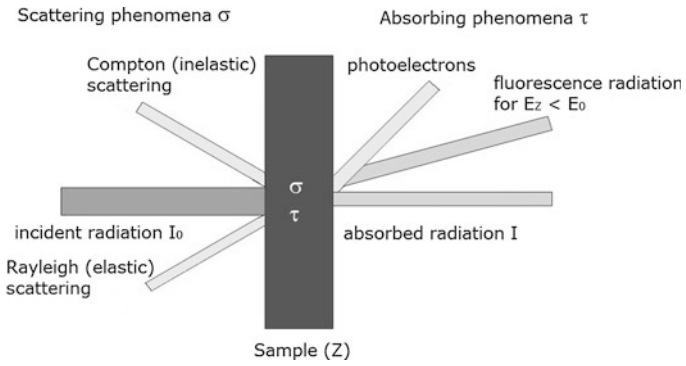

Fig. 1.1 Interactions of X-rays

1.2.1 Absorption

If X-rays incident into material with atomic number Z they interact with the material and will be attenuated. This interaction is described by the mass absorption μ. The mass absorption is the sum of absorption and scattering which are described by τ and σ, respectively. The contribution of scattering to attenuation is relatively small that means

$$\mu = \tau + \sigma \quad \text{can be written as} \quad \mu \approx \tau \tag{1.1}$$

The absorption can be described by the Lambert-Beer-law. That means the intensity of the incident radiation will be decreased. The absorption depends on the mass attenuation coefficient μ, the density of the material ρ and the thickness of the material t.

$$I = I_o \exp(-\mu \cdot \rho \cdot t) \tag{1.2}$$

with

I_o primary intensity
μ mass attenuation coefficient as function of energy
ρ density of the absorbing material
t thickness of the absorbing layer

The mass attenuation coefficient depends on the radiation energy i.e. $\mu = \mu(E)$. If the material is composed of different elements the mass attenuation coefficient can be calculated as the average

$$\mu_{compound} = \sum w_i \mu_i \tag{1.3}$$

with
w_i mass fraction of element i
μ_i mass absorption coefficient of element i

This interaction was the first which was seen by Roentgen itself. The image of his hand with a ring is well known. X-ray absorption is often used for medical applications. X-rays penetrate for example the human body but will be different absorbed in the bones and tissue. This allows the generation of images of the bones and the different tissues, particularly when materials of heavy elements that are injected into the blood's circulation system or into the alimentary tract cause greater contrast between the differing tissues and organs.

But very soon this interaction was also used for the analysis of inorganic materials. The first target was a 2-dimensional imaging of the material for the investigation of its internal structure, for example, the identification of inclusions like blow holes or cracks in metals. If the X-ray source is a point source it is even possible to adjust the image size by changing of the distances between X-ray source, sample and detector. Then the image can be magnified which simplifies the image post-processing.

But then, with the availability of more computing power it was also possible to generate 3-dimensional images due to the collection of absorption images in different directions and their reconstruction to a complete model of a specimen—this is called X-ray tomography. Tomography can be performed for large bodies like technical design elements by using tube voltages in the range up to 350 kV. It can be done for the human body with tube voltages in the range up to 150 kV but also for small grains, particles or films with tube voltages in the range up to 80 kV. The reconstruction generates a 3-dimensional model of the investigated material with possibilities to prepare cross sections in different directions or semi-transparent models to show all interesting details.

For all these absorption applications the energy of X-rays has to be adapted to the size of the analyzed sample and to their matrix to have a sufficient dynamic range of the signal. The energy of the X-rays needs to be large enough to penetrate the sample that should be analyzed but there should be also a sufficient absorption that a change of the signal can be detected.

One of the latest applications of X-ray absorption is a real X-ray microscopy [49–53]. In that case the sample is illuminated with X-rays and the absorbed radiation will be magnified by using X-ray optics with a similar beam path as in optical microscopes. Typically Fresnel-lenses are used for that purpose. They can magnify the image of the examined sample. The magnification depends on the structure of the Fresnel-lenses—in particular from the dimensions of the outer ring of the optic. So far the spatial resolution is limited to the range of approx. 20 nm. Due to the high absorption this technique can be used in the moment only for light materials like organic materials.

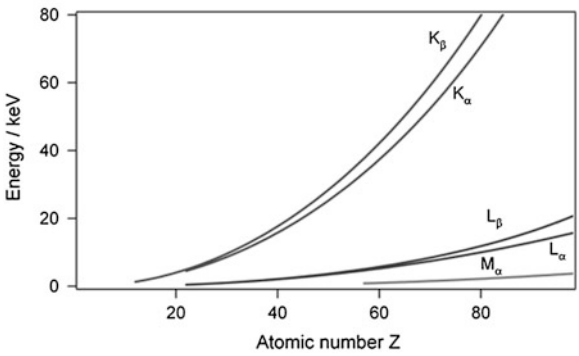

Fig. 1.2 Dependence of the energy of characteristic radiation from atomic number

1.2.2 Emission of Fluorescence Radiation

The absorption process of X-rays in matter can generate phonons i.e. enhance the oscillations of the lattice or they excite atoms by the emission of a photo-electron. Due to the high energy of the incident X-ray this electron can come even from the inner shells of the atom. If the vacancy in this shell is filled up by outer electrons the atom is going into the ground state and energy can be emitted as electromagnetic radiation. This radiation has typically energies in the range of X-rays. This process is called X-ray fluorescence because it can be excited by radiation or it can be called also emission of characteristic radiation because their energies are characteristic for the involved atom [54–59, 60]. Moseley [61, 62] found in 1913 that there is a relation between the energy of characteristic radiation E and the atomic number Z of the emitting atom which is called now Moseley's law:

$$E = C_1 \cdot (Z - C_2)^2 \tag{1.4}$$

with:C_1, C_2 constants which depends on the involved electron shells.

This relation is presented in Fig. 1.2. It shows the energy of characteristic radiation in dependence of atomic number Z for all X-ray series (K, L and M).

The intensity of emitted radiation depends on the intensity of excitation radiation and the absorption of the material i.e. the mass attenuation coefficient μ. But this describes only the generation of a vacancy in an inner electron shell. This vacancy has to be filled from an outer electron which is described by its transition probability p which is different for the various transitions. The energy difference between the binding energy of the two electron shells $E_{diff} = E_{vacancy} - E_{outer}$ of this transition can be emitted directly by an X-ray which is the characteristic radiation.

Another possibility is the emission of an Auger-electron [63]. In that case the energy E_{diff} is transferred within the atom to an outer electron which left the atom with the energy $E_{Auger} = E_{diff} - E_{binding}$. Because only one process for the

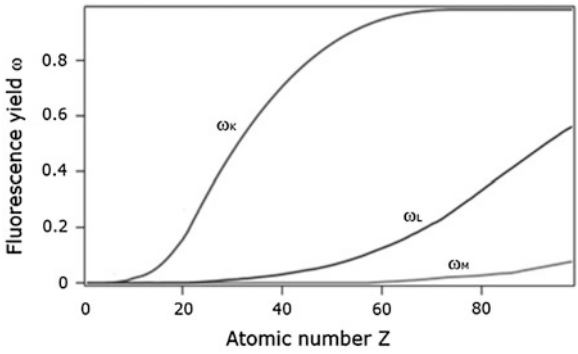

Fig. 1.3 Fluorescence yield in dependence of energy

energy emission is possible, the probability for their sum needs to be unit i.e. $p_{Auger} + p_{X\text{-}ray} = 1$. The probability for an X-ray emission is called fluorescence yield ω and depends on energy and the electron transition as shown in Fig. 1.3.

The emission of characteristic X-rays can be used for the determination of elemental composition of samples but also for the analysis of coating systems according to their thickness and composition.

In addition to the characterisitic radiation with discrete energies there is also a continuous radiation in the energy range of X-rays. This is called bremsstrahlung according to its generation process (for a more detailed decription see 2.1.1). This possibility of X-ray fluorescence was used already very early for elemental analysis. The first instruments were built in the 30th of the last century for the analysis of homogeneous samples [64, 65]. Typical applications were in metallurgy and in mining.

The special advantage of X-ray fluorescence is the good repeatability and reproducibility i.e. their high precision. The high precision is result of the small contribution of statistical errors caused by the high count rate. Another benefit is the wide range of weight fractions that can be covered with XRF.

These exceptionally useful aspects of XRF mean it is now used in countless laboratories for a large variety of applications. Several generations of X-ray fluorescence spectrometers have been developed and used. Nowadays there are different types of X-ray spectrometers available which can be used for different analytical tasks:

- The detection of fluorescence radiation allows on the lowest level the determination of the elements that have emitted this radiation i.e. a qualitative analysis.
- The peak intensity of every peak depends on the amount of atoms of this element in the analyzed volume. This allows the calculation of the weight fractions of existing elements. The weight fraction range covered by XRF depends on the used method but can be very large—up to 6 orders of magnitude. It depends also on the examined element. Very light elements cannot be analyzed due to the very low energy of their characteristic radiation.

- Accuracy requirements are also different—it ranges from the control of levels of weight fractions to their accurate determination with the help of references or even with bracketing procedures.
- The sample quality can vary from liquids to powders and solid samples, also the analysis of material streams are possible.
- In case of layer systems the peak intensity depends on the layer thickness. For the analysis of layer systems further knowledge about the structure of the layer system is necessary.

1.2.3 Refraction

The refraction index n in the energy range of X-rays can be written as:

$$n = 1 - \delta + i\beta \tag{1.5}$$

with
δ deviation from 1 (approx. 10^{-6}–10^{-7})
β absorption coefficient

This shows the refraction index for X-rays is for all materials very close to 1. It depends mainly on the density. Therefore differences between refraction indices for X-rays in different materials are very small and their refraction is negligible. Further it can be seen that all refraction indices are negative. That means the very small refraction is in direction of the higher density and according to Snellius's law total reflection happens for X-rays only for very small incident angles and materials with higher density.

X-ray refraction is not used for material characterization but for X-ray optics refraction is an important process which can be used for beam shaping (see Sect. 2.2.3).

1.2.4 Scattering

X-rays are scattered on electrons. This scattering can be described by the classical electromagnetic theory as well as with the particle model for the X-ray photon. Both descriptions give different behaviors of the scattered X-rays.

The electromagnetic theory describes an elastic scattering i.e. without a loss of energy of the scattered X-ray [66, 67]. This scattering is also called coherent or Rayleigh-scattering. For randomly distributed directions of the electromagnetic field of the X-rays the scattering can be described by the Rayleigh formulae:

$$I_{scat} = I_0 \frac{1}{r^2} \left(\frac{e^2}{m_0 c^2} \right)^2 \cdot (1 + \cos^2 \vartheta) \tag{1.6}$$

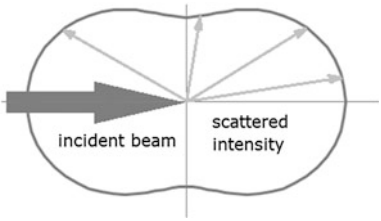

Fig. 1.4 Dependence of Rayleigh-scattering intensity from the scattering angle

with

I_{Scat}	scattered intensity
I_0	primary intensity
r	distance to the observation point
e	charge of an electron
m_0	mass of an electron
ϑ	scatter angle

This formula shows no change of energy but a dependence from the scatter angle. In Fig. 1.4 this dependence is displayed in polar-coordinates i.e. the scatter intensity is presented as the distance from the point of origin (incident point of the radiation) in every direction.

For scattering angles Θ close to 0° or 180° i.e. in forward or backward direction the scattered intensities is high but for scattering with angles close to 90° i.e. scattering perpendicular to the incident beam the scattered intensity has a minimum.

By using the corpuscular image for the description of the scattering the X-ray photon hits an electron. Due to that hit the photon transfers energy and momentum to the electron. For that process both energy and momentum conservation is valid. Therefore the energy loss of the photon depends on the on its scatter angle. Because the scattered photon has lost energy it is called inelastic scattering or also incoherent or Compton-scattering [68]. Due to the loss of energy the wavelength of the photon is increased. The wavelength of the scattered radiation λ_{scatt} can be described as follows:

$$\lambda_{scatt} = \lambda_0 + \lambda_C \cdot (1 - \cos\vartheta) \tag{1.7}$$

with

$\lambda_c = h/mc$	Compton wavelength
m	mass of the scattering particle, here an electron
λ_0	wavelength of the incident photon
ϑ	scatter angle

For an energy dispersive spectrometer it is easier to calculate the change of energy which can be written as:

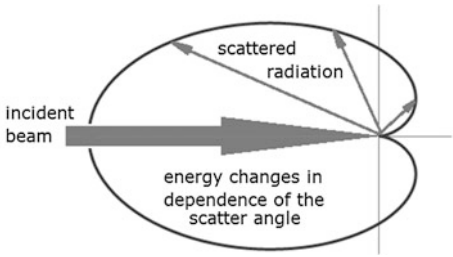

Fig. 1.5 Dependence of the Compton-shift from the scattering angle

$$E_{Scatt} = \frac{E_0}{1 + \frac{1}{mc^2} \cdot (1 - \cos \vartheta)} \tag{1.8}$$

with:
E_0 energy of incident radiation.
This formula shows that the energy loss of the photons depends on the energy of the incident photon and on the scattering angle. The dependence of the energy change $E_0 - E_{scatt}$ on the scattering angle is displayed in Fig. 1.5—again in polar-coordinates i.e. the energy change is displayed as the distance from the origin in every scatter direction. It shows that for scatter angles close to 0° i.e. if the photons don't hit the electron there is no loss of photon energy. For small scattering angles only a small fraction of the photon energy is transferred to the electron. The largest energy loss happens in case of a direct hit of the photon with the electron i.e. for a scattering angle close to 180°. Then a large fraction of the photon energy is transferred to the electron and the Compton shift has a large value.

This behavior is demonstrated in Fig. 1.6 which shows the scattered tube radiation on a Plexiglas sample (PMMA) for two scatter angles in backward direction. The blue spectrum had an angle between tube and detector of 78° i.e. a scatter angle of 102°, for the red spectrum the scatter angle is 128°.

The spectra show that both elastic and inelastic scattering are responsible for the spectral background. The elastic scattered fluorescence radiation of the tube (Rh) can be seen in the spectrum as narrow peaks both for K- and L-radiation. The large peak in front of the Rh-K-line is the Compton-scattered K-line. This Compton-peak is less shifted towards lower energies for the smaller scattering angle (blue spectrum). But this dependence is valid not only for the fluorescence radiation of the tube but also for their bremsstrahlung. This can be seen by a comparison of the slope of the bremsstrahlung—also this shows a larger shift for the larger scatter angle. Further the energy dependence of the Compton shift can be seen—for the Rh-Kα line at 20.2 keV it is smaller than for the Rh-Kβ-line at 22.8 keV.

The Rh-L-radiation is not Compton scattered because the energy is too small and the scattering probability is reduced (see Fig. 1.8).

That these shifts are only valid for scattered radiation can be seen on the Zr-peak which is excited on the detector collimator and is therefore not Compton shifted.

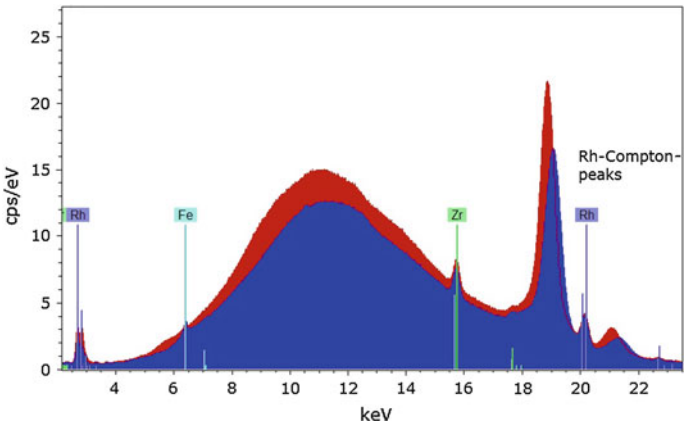

Fig. 1.6 Scattered tube spectra with scatter angles of 102° (*blue*) and 128° (*red*)

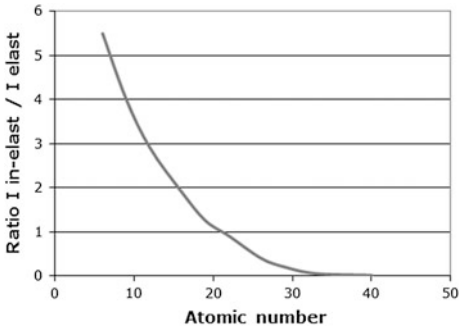

Fig. 1.7 Compton-Rayleigh ratio in dependence of average atomic number of the matrix

The inelastic scattered Compton-peak has a significant larger FWHM which is a result of the movement of the scattering electrons which causes a Doppler-broadening of the scattered peak [67].

The scattering intensities of the elastic and the inelastic scattering depend on the matrix, in particular on the average atomic number of the matrix. Whereas the elastic scattering is widely independent of the matrix the inelastic scattering depends on the matrix. The relation between the intensities of Rayleigh and Compton scattering in dependence of the average atomic number of the sample is shown displayed in Fig. 1.7. It can be seen that the inelastic scattering for light matrices has a larger intensity and drops down for increasing atomic numbers. This relation can be used for the determination of the average atomic number of the matrix or of the fraction of dark matrix in a sample [69].

Absorption and scattering attenuate X-rays if they penetrate material. Their contributions can be described by their cross sections. As an example the cross sections for the different attenuation processes for Silicon in dependence of energy are displayed in Fig. 1.8.

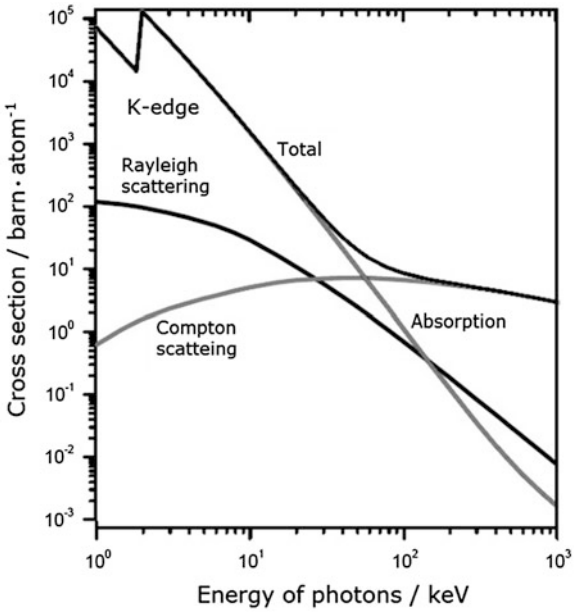

Fig. 1.8 Different contributions to X-ray cross section of Si

For the energy range that is interesting for X-ray spectroscopy i.e. from 1 to 40 keV absorption is dominating. For low energies the Rayleigh scattering is 3 orders of magnitude smaller than absorption but Compton scattering even 5 orders of magnitude. For higher energies—at approximately 30 keV the scattering cross section are comparable and at approximately 60 keV they have an even higher probability than absorption.

Scattered X-rays are also used for material characterization. So it is possible to use the scattering at small angles for the determination of short range order structures.

1.2.5 Diffraction

Immediately after the discovery of X-rays scientists starts to examine this new type of radiation. Laue and co-workers found 1912 that X-rays are scattered on crystals [70]. This could be interpreted as an interference of scattered X-rays on the periodically structure of the crystal. Further investigations of this scattering behavior brought father and son Bragg the cognition of their scattering law [71]:

$$n \cdot \lambda = 2d \cdot \sin \vartheta \tag{1.9}$$

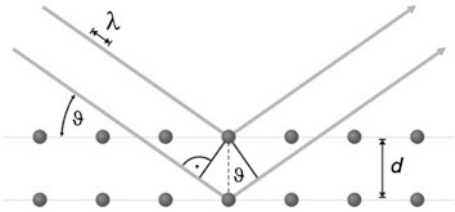

Fig. 1.9 Explanation of the Bragg law

Table 1.1 Use of Bragg's-law for material investigation

Method	Fixed	Measured	Calculated
XRD	λ or E	ϑ	d
WDX	d	ϑ	λ
ED-XRD	ϑ	E	d

with

λ wavelength of the scattered radiation
d d-spacing of the scattering lattice
ϑ scatter angle

This relation can be understood from Fig. 1.9. The incident radiation is coherent scattered on the electrons of the lattice atoms. The scattered waves of the different atoms interfere and can amplify or annihilate each other in dependence of their path length differences. If the path length is a multiple n of the wavelength λ the overlapping of the waves generates high intensity reflections at the scatter angle ϑ.

This diffraction of X-rays finally explained the nature of X-rays but opened also the possibility for investigations of the structure of material [72–76].

The Bragg-relation offers different possibilities for material investigation. It has three parameters. If one of them is fixed and another is measured, the third one can be calculated. The different possibilities for using that relation for material analysis are summarized in Table 1.1.

With XRD it is possible to examine the symmetry of single crystals and explain their structure and it is possible to study the structure of powders and polycrystalline materials to understand their mechanical behavior [73–75]. With ED-XRD it is possible to look for individual diffraction peaks and control fast changes of their intensity due to structural changes and with WDX the spectroscopic investigation of spectra is possible allowing, for example, the analysis of characteristic radiation of material and in this way the determination of its elemental composition.

1.3 General Design of X-ray Spectrometers

All X-ray spectrometers have a similar design with the same main components. The intended analytical task defines the use of the different components and their requested parameters. A general design with the main components is presented in Fig. 1.10.

The following main components are required:

- ***Excitation source***

In laboratory instruments the excitation is performed mostly with an X-ray tube. But also the excitation with radioactive sources in transportable instruments or with synchrotrons for highly sophisticated investigations is common. Direct excitation with electrons is mostly used in electron microscopes.

- ***Primary optic***

Primary optics are used to change the energy distribution of the radiation or perform a beam shaping. Changes of the energy distribution are possible with filters, secondary targets or monochromators, the shape of the excitation beam can be influenced by collimators or X-ray optics. Often with X-ray optics both shape and energy distribution of the beam are influenced.

- ***Sample positioning system***

The sample needs to be positioned in the beam. For spectrometers that analyze large sample areas this is often only a sample cup that will be positioned with a sample tray. For position-sensitive analysis manual or motorized sample positioning in X and Y is possible. Then the sample position often is controlled by an optical microscope.

- ***Secondary optic***

The secondary optic can be very complex. It can be required as a beam shaper which improves resolution or peak-to-background ratio but it can be also a dispersive optic that is used as (variable) monochromator.

- ***Detector***

The detector measures the photons coming from the sample. For a WDX instrument the detector needs only to count the photons because the dispersion is performed in the secondary optic. In the case of energy dispersive detectors the detector makes the dispersion as well as counting. Therefore there are different detectors that have also different counting behaviors.

Additional to the mentioned components some further components are required for a complete spectrometer—X-rays are ionizing radiation and can damage the human tissue, therefore the complete spectrometer should be shielded against accidental radiation of the environment, in particular of humans. Further the different component settings need to be operated and the data acquisition needs to be controlled. For that purpose nowadays, all instruments are operated by processors. Often the measurement has to be performed in a special medium: vacuum, He or air which has to be supplied by pump, flushing systems etc. All these components are important for the analytical performance but don't are main components of the

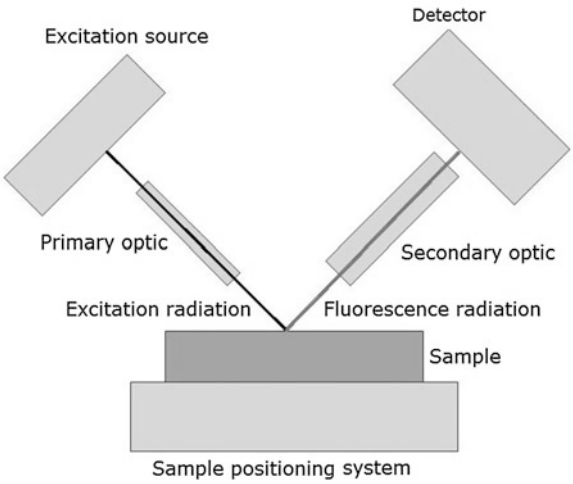

Fig. 1.10 Scheme of the main components of an X-ray spectrometer

instrument. Last, but not least, the acquired data has to be evaluated. This requires often complex calculations. Also for that purpose microprocessors are used.

The main components can be very different. Their parameters determine the performance of the spectrometer and their design depends on the analytical task.

References

1. F.R. Elder, A.M. Gurewitsch, R.V. Langmuir, H.C. Pollock, Phys. Rev. **71**, 829 (1947)
2. E.E. Koch, D.E. Eastman, Y. Farge, *Handbook of Synchrotron Radiation*, vol. 1A (North Holland Publishing Company, Amsterdam, 1983), p. 1
3. P. Horowitz, J. Howell, Science **178**, 608 (1972)
4. C.J. Sparks, S. Raman, H.L. Yakel, R.V. Gentry, M.O. Krause, Phys. Rev. Lett. **38**, 208 (1977)
5. K.W. Jones, in *Handbook of X-Ray Spectrometry*, ed. by R.E. van Grieken, A.A. Markowitz (Marcel Dekker, New York, 1992), p. 411
6. B. Gordon, K.W. Jones, in *Microscopic and Spectroscopic Imaging of the Chemical State*, ed. by M.D. Morris (Marcel Dekker, New York, 1993)
7. K.W. Jones, B. Gordon, Anal. Chem. **61**, 341 (1989)
8. S. Hayakawa, A. Iida, Y. Goshi, Rev. Sci. Instrum. **60**, 24 (1989)
9. R.D. Vis, F. van Langefelde, Nucl. Instr. Meth. **B54**, 417 (1991)
10. M.L. Rivers, S.R. Sutton, Synchrotron Radiat. News **4**, 223 (1991)
11. A.C. Thomson, K.L. Chapman, C.E. Sparks, W. Yun, D. Lai, D. Legini, P.J. Vicaro, M.L. Rivers, D.H. Bilderback, D.J. Thiel, Nucl Instr. Meth **A319**, 320 (1992)
12. F. Lechtenberg, S. Garbe, J. Bauch, D.B. Dingwell, J. Freitag, M. Haller, T.H. Hansteen, P. Ippach, A. Knöchel, M. Radtke, C. Romano, P.M. Sachs, H.U. Schmincke, H.J. Ullrich, J. Trace Microprobe Tech. **14–3**, 561 (1996)
13. P. Chevallier, P. Dhez, F. Legrand, A. Erko, Y. Agafonov, L.A. Panchanko, A. Yakshin, J. Trace Microprobe Tech. **14–3**, 517 (1996)

14. K. Janssens, L. Vincze, B. Vekemans, F. Adams, M. Haller, A. Knöchel, J. Anal. At. Spectr. **13**, 339 (1998)
15. G. von Hevesy, *Chemical Analysis by X-Rays and Its Application* (McGraw Hill, New York, 1932)
16. R. Glocker, H. Schrieber, Ann. Phys. **85**, 130 (1928)
17. M.A. Blokhin, *Methods of X-Ray Spectroscopic Research* (Pergamon press, New York, 1965)
18. R. Jenkins, J.L. de Vries, *Practical X-ray Spectrometry* (McMillan, London, 1967)
19. I. Adler, J. Axelrod, J.J. Branco, Adv. X-Ray Anal. **5**, 2 (1962)
20. H.J. Rose, R.P. Christian, J.R. Lindsay, R.R. Larson, Geol. Surv. Proj. Pap. (US) **650**, 8128 (1969)
21. M.C. Nichols, D.R. Boehme, R.W. Ryon, D. Wherry, B.J. Cross, G. Aden, Adv. X-Ray Anal. **30**, 45 (1987)
22. R. Ryon, H.E. Martz, J.M. Hernandez, B.J. Cross, D. Wherry, Adv. X-Ray Anal. **31**, 35 (1988)
23. C.D. Wherry, B.J. Cross, T.H. Briggs, Adv. X-Ray Anal. **31**, 93 (1988)
24. D.B. Wittry, in *Proceedings of the 50th Annual Meeting of the Electron Microscopy Society of America (EMSA/MAS)*, Boston, (1992)
25. R.G. Tissot, D.R. Boehme, Paper presented on 42nd Denver Conference on Applications of X-Ray Analysis, (Book of abstracts, 1993), p. 152
26. G.J. Havrilla, Paper presented on 42nd Denver Conference on Applications of X-Ray Analysis, (Book of abstracts, 1993), p. 153
27. M.C. Nichols, R.W. Ryon, Adv. X-Ray Anal. **29**, 423 (1986)
28. E. Spiller, A. Segmuller, Appl. Phys. Lett. **27**, 101 (1974)
29. D. Mosher, S.J. Stephanakis, Appl. Phys. Lett. **29**, 105 (1976)
30. A. Rindby, Nucl. Instr. Meth. **A249**, 536 (1986)
31. D.A. Carpenter, X-Ray Spectrom. **18**, 253 (1989)
32. D.A. Carpenter, M.A. Taylor, C.E. Holcombe, Adv. X-Ray Anal. **32**, 115 (1989)
33. D.A. Carpenter, M.A. Taylor, Adv. X-Ray Anal. **34**, 217 (1981)
34. Y. Yamamoto, Y. Hosokawa, Jpn. J. Appl. Phys. **27**, 2203 (1988)
35. A. Rindby, P. Engström, K.H. Janssens, J. Osan, Nucl. Instr. Meth. **124B**, 591 (1997)
36. Y. Yinming, X. Ding, Nucl. Instr. Meth. **82B**, 121 (1993)
37. M. Haschke, W. Scholz, U. Theis, in *Proceedings of EDXRF Conference*, Bologna, 1998, p. 157
38. S. Bichlmeier, K.H. Janssens, J. Heckel, D. Gibson, P. Hoffmann, H.M. Ortner, X-Ray Spectr. **30**, 8 (2001)
39. M. Haschke, W. Scholz, U. Theis, J. Nicolosi, B. Scruggs, L. Herczeg, J. de Phys. IV **12**, 83 (2002)
40. A.A. Bzhaumikhov, N. Langhoff, J. Schmalz, R. Wedell, V.I. Beloglazov, N.F. Lebedev, in *Proceedings of SPIE*, vol. 3444 (1998), p. 430
41. B. Holynska, J. Ostachowicz, A. Ostrowski, D. Ptasinski, D. Wegrzynek, J. Trace Microprobe Tech. **13**, 163 (1995)
42. A. Longoni, C. Fiorini, P. Leutenegger, L. Sciuti, G. Fronterotta, L. Strüder, P. Lechner, Nucl. Instr. Meth. **409**, 407 (1998)
43. R.D. Evans, *The Atomic Nucleus* (McGraw-Hill, New York, 1955)
44. J.M. Jauch, F. Rohrlich, *The Theory of Photons and Electrons*, 2nd edn. (Springer, Berlin, 1976)
45. B.K. Agarwal, *X-ray Spectroscopy: An Introduction*, (Springer, Berlin, 1991). ISBN 0-387-092684
46. E.P. Bertin, *Priciples and Practice of X-ray Spectrometric Analysis* (Plenum Press, New York, 1975)
47. P. Hahn-Weinheimer, A. Hirner, K. Weber-Diefenbach, *Röntgenfluoreszenz-analytische Methoden, Grundlagen und praktische Anwendung in den Geo-. Material- und Umweltwissenschaften* (Springer, Berlin). ISBN-10: 3540670211

48. R. Jenkins, R.W. Gould, D. Gedcke, *Quantitative X-ray Spectrometry* (Marcel Dekker Inc., New York, 1981). ISBN 8: 0-8247-1266-8
49. G. Schmahl, D. Rudolph, in *Proceedings of the International Symposium Göttingen* (Springer, 1984)
50. G. Schneider, *High-Resolution X-ray Microscopy of Radiation Sensitive Material* (Cullivier, 1999)
51. H. Legall, G. Blobel, H. Stiel, W. Sandner, C. Seim, P. Takman, D.H. Martz, M. Selin, U. Vogt, H.M. Hertz, D. Esser, H. Sipma, J. Luttmann, M. Höfer, H.D. Hoffmann, S. Yulin, T. Feigl, S. Rehbein, P. Guttmann, G. Schneider, U. Wiesemann, M. Wirtz, W. Diete, Opt. Express **20–6**, 18362 (2012)
52. P.A.C. Takman, H. Stollberg, G.A. Johansson, A. Holmberg, M. Lindblom, H.M. Hertz, J. Microsc. **226–2**, 175 (2007)
53. http://www.xradia.com
54. J.H. Scofield, Trans. Am. Nucl. Soc. **55**, 200 (1987)
55. J.A. Bearden, Rev. Mod. Phys. **39**, 78 (1967)
56. C.G. Barkla, C.A. Sadler, Phil. Mag. **16**, 550 (1908)
57. H.J. Beattie, R.M. Brissey, Anal. Chem. **26**, 980 (1954)
58. R.T. Beatty, Proc. R. Soc. Lond. **A87**, 511 (1912)
59. H.A. Kramers, Phil. Mag. **46**, 836 (1923)
60. M. Siegbahn, *The Spectroscopy of X-rays* (Oxford University Press, London, 1925)
61. H.G.J. Moseley, Phil. Mag. **26**, 1024 (1913)
62. H.G.J. Moseley, Phil. Mag. **27**, 703 (1914)
63. P. Auger, J. Phys. et Le Radium **6**, 205 (1925)
64. G. von Hevesy, *Chemical Analysis by X-rays and Its Applications* (McGraw-Hill, New York, 1932)
65. R. Glocker, H. Schreiber, Ann. Phys. **85**, 1089 (1928)
66. J.J. Thomson, G. Thomson, *The Conduction of Electricity Through Gases*, 3rd edn. (Cambridge University press, Cambridge, 1933)
67. D.V. Rao, T. Takeda, Y. Itai, T. Akatsuka, R. Cesareo, A. Brunetti, G.E. Gigante, J. Phys. Chem. Data **31–3**, 769 (2002)
68. A.H. Compton, Phys. Rev. **21–5**, 483 (1923)
69. K. Molt, R. Schramm, X-Ray Spectr. **28**, 59 (1999)
70. W. Friedrich, P. Knipping, M. von Laue, Interferenz-Erscheinungen bei Röntgenstrahlen, in *Bayerische Akademie der Wissenschaften, Sitzungsberichte* (1912), p. 303
71. H. Bragg, W.L. Bragg, Proc. R. Soc. Lond. **A 88**, 428 (1913)
72. P. Debye, P. Scherrer, Nachr. Ges. Wiss. Göttingen, Mathematisch-Physikalische Klasse 1 (1916)
73. W. Kleber, *Einführung in die Kristallographie* (VEB Verlag Technik, Berlin, 1969)
74. W.H. Zachariasen, *Theory of X-ray Diffraction in Crystals* (Dover Publications, New York, 1967)
75. W. Clegg, *Crystal Structure Determination* (Oxford University Press, Oxford Chemistry Primer, 1998)
76. W. Massa, *Crystal Structure Determination* (Springer, Berlin, 2004)

http://www.springer.com/978-3-319-05316-5

Geometric Theory of Information
Nielsen, F. (Ed.)
2014, XII, 392 p. 81 illus., 60 illus. in color., Hardcover
ISBN: 978-3-319-05316-5